HUNGARIAN UNIVERSITY OF AGRICULTURE AND LIFE SCIENCES

Performance analysis of a parabolic trough solar collector

PhD Thesis

by

Asaad Yasseen Al-Rabeeah

Gödöllő

2023

Doctoral school

Denomination: Doctoral School of Mechanical Engineering

Science: Mechanical Engineering

Leader: Prof. Dr. Gábor Kalácska, DSc
Institute of Technology
Hungarian University of Agriculture and Life Sciences,
Gödöllő, Hungary

Supervisor: Prof. Dr. István Farkas, DSc
Institute of Technology
Hungarian University of Agriculture and Life Sciences,
Gödöllő, Hungary

Co-Supervisor: Dr. István Seres, PhD
Institute of Mathematics and Basic Science
Hungarian University of Agriculture and Life Sciences,
Gödöllő, Hungary

…………………………………   …………………………………
Affirmation of supervisor   Affirmation of head of school

CONTENTS

1. INTRODUCTION, OBJECTIVES

The parabolic trough solar collector (PTSC) technology is one of the most reliable technologies in the field of solar thermal. It is mainly used for power generation (e.g., generating steam, which needs high temperatures) and other technological purposes. The collectors receive direct solar radiation from the sun over a large surface and gather it to the focal point. The PTSC consists of a reflector surface in a parabolic shape that concentrates the solar radiation into a receiver tube that transports a working fluid.

Several parameters have effects on PTSC performance, such as the mass flow rate of the working fluid, ambient temperature, and the incident angle of the solar radiation, which increase and decrease heat losses. A fluid flowing inside the tube absorbs the heat energy generated from the focused solar radiation, raising its enthalpy, and causing an increase in the temperature of the tube wall.

A working fluid is an essential component for enhancing the efficiency of PTSCs. The mixing of nanoparticles with the working fluid is an effective method of increasing the collected thermal energy and the nanofluids' thermophysical properties. The thermal efficiency of PTSC depends on the concentration of the volume fraction of nanoparticles in the base fluid. Proper design and using nanofluid for optimization of heat flux distribution are key matters on enhancing performance of PTSC and improving economic advantages the entire system, the main objectives of the present work are to investigate the following:

- To experimentally determine the thermal conductivity of mono and hybrid nanofluids at different concentrations and temperatures.

- To experimentally study the effect of the viscosity of mono and hybrid nanofluids at different temperatures and concentrations.

- To study the effect of nanofluids as working fluids on the efficiency and operation of the PTSC system.

- To validate the ANSYS simulation models with experimental results that describing the heat and mass transfer processes of the PTSC system at traditional working fluids compared with mono and hybrid nanofluid.

- To experimental analysis and comparison of the efficiency of the PTSC under different receiver tubes and different mass flow rates.

- To study the different selective coatings to enhance PTSC performance.

- To study the effect of two different reflecting surfaces, one made of silver-chrome film and the other of aluminium to enhance the efficiency of the PTSC.

2. MATERIALS AND METHODS

This chapter covers the description of the materials, techniques, and equipment used, as well as the scientific methodologies employed in the experimental measurements to accomplish the research goals.

2.1. Description and experimental set up

Two similar prototype PTSCs were made and tested in Gödöllő city at the Hungarian University of Agriculture and Life Sciences, Solar Energy Laboratory. Moreover, the information is checked by the parabolic equations of mathematics, which are described as follows:

The concentration ratio is calculated by dividing the area of the collector aperture by the area of the absorber:

$$C = \frac{A_a}{A_{ro}}. \tag{1}$$

The useful heat from the PTSC can be calculated based on the difference in the temperature of fluid that flows through the receiver tube, according to the following equation:

$$Q_u = \dot{m} \ c_p (T_{out} - T_{in}). \tag{2}$$

The solar irradiation on the collector aperture (Q_s) can be calculated by multiplying the aperture area by the direct beam solar irradiation as follows:

$$Q_S = A_a \times I_b. \tag{3}$$

The thermal efficiency of PTSC is calculated by the ratio of useful heat to available direct beam radiation:

$$\eta_{th} = \frac{Q_u}{Q_s}. \tag{4}$$

The thermal efficiency of PTSC can be calculated using this equation as a linear equation:

$$\eta_{th} = a + bT^*, \tag{5}$$

where (a) is the absorbed energy parameter, and calculated as follows:

$$a = F_r \eta_o \tag{6}$$

where (b) is the parameter for the removal of energy (slope):

$$b = -\frac{F_r U_L}{C}, \tag{7}$$

where (T^*) is the heat loss parameter:

$$T^* = \left(\frac{T_{in} - T_{amb}}{I_b} \right), \tag{8}$$

F_r represents the ratio of the actual useful energy to the maximum useful gain.

2. Materials and methods

The optical efficiency of a PTSC is the ratio of energy absorbed by the receiver to that collected by the aperture. The following formula is used to obtain get the PTSC's optical efficiency.

$$\eta_o = \rho\tau\alpha\gamma. \tag{9}$$

Besides, Fig. 1 presents the hydraulic cycle that was used in the process of analysing the thermal efficiency of the PTSC system. Fig. 2 presents the experimental work done, which is the same as the ANSYS model.

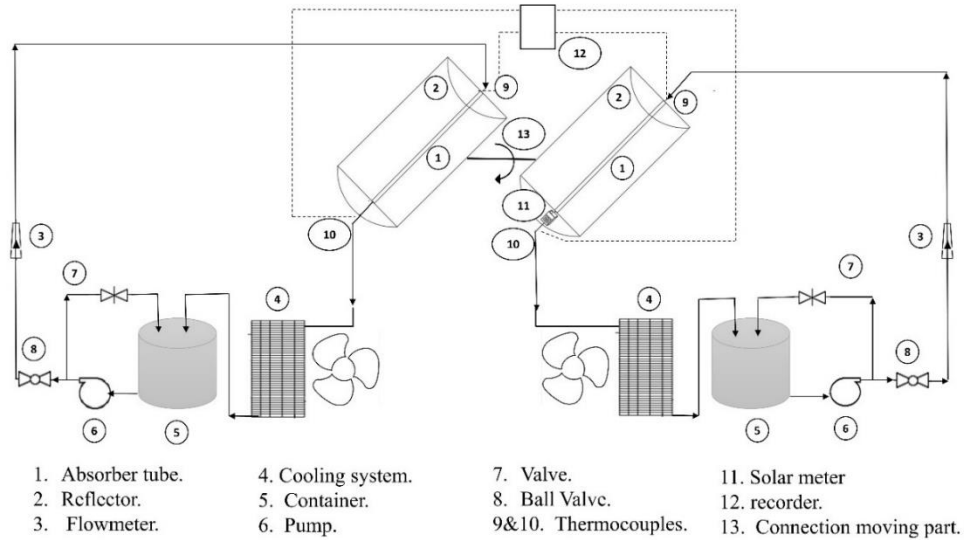|			
1. Absorber tube.	4. Cooling system.	7. Valve.	11. Solar meter
2. Reflector.	5. Container.	8. Ball Valve.	12. recorder.
3. Flowmeter.	6. Pump.	9&10. Thermocouples.	13. Connection moving part.

Fig. 1. Model demonstration

Fig. 2. Experimental setup

2.2. Preparations of hybrid Nanofluids

The nanofluids (NFs) used in this study were prepared using a two-step method. The two-step process is the most economical way to produce nanofluids in large quantities. Four volume concentrations (VCs) of hybrid nanofluids (HNFs) were prepared: 0.01%, 0.05%, 0.1%, and 0.2% nanofluids. The NF was prepared using a mixing ratio of 1:1 graphene to Fe_3O_4 of nanoparticles with water as the base fluid and adding Gum Arabic surfactant. The NFs were placed in a beaker (200 mL) and stirred for 1 hour, followed by 2.5 h of ultrasonic mixing to break down agglomeration between particles and produce uniform dispersion in the base fluid to create a stable NF. According to the experimental results, the thermal conductivity ratio (TCR) and thermal conductivity enhancement (TCE) are defined in as follows:

$$TCR = \frac{k_{nf}}{k_{bf}}. \tag{10}$$

$$TCE(\%) = \frac{k_{nf} - k_{bf}}{k_{bf}} \times 100. \tag{11}$$

Fig. 3 shows that the thermal conductivity (TC) of NF increases with particle concentrations and temperatures. The variations in HNF viscosity as a function of nanoparticle volume concentration and temperature are represented in Fig. 4.

$$RV = \left[\frac{\mu_{nf}}{\mu_{bf}}\right]. \tag{12}$$

The viscosity of the NF decreased when the temperature was increased from 20 °C to 60 °C at the constant VC. Increases in temperature reduce viscosity due to decreased adhesion forces and Brownian motion.
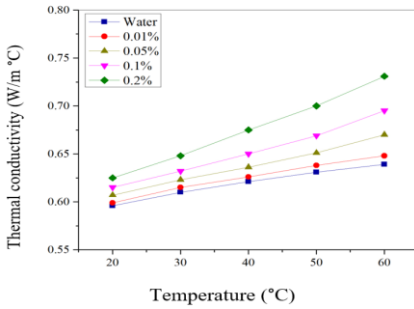

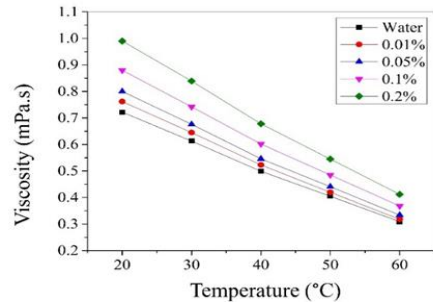Fig. 3. TC of HNF with (a) VCs at different temperatures

Fig. 4. The viscosity at different temperatures and VCs.

Further, a new proposed correlation was obtained to measure the thermal conductivity ratio and viscosity variations at different concentrations and

temperatures, we determined the TCR and RV by using Eqs. 13 and 14 at different temperatures as follows:

$$TCR = 0.9994 + 0.05436\,\varphi + 0.00012\,T - 0.4568\,\varphi^2 + 0.01178\,\varphi\,T. \qquad (13)$$

$$RV = 1.044 + 1.889\,\varphi - 0.0006066\,T - 0.6786\,\varphi^2 - 0.001685\varphi\,T. \qquad (14)$$

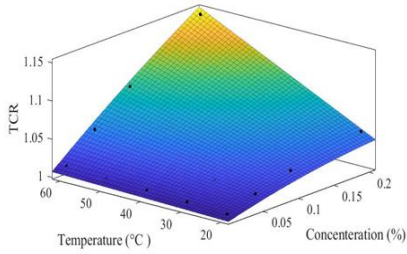Figs. 5 and 6 show a comparison between the experimental results obtained and the proposed equation.

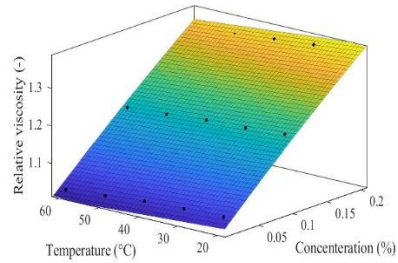Fig. 5. TCR comparisons for different temperatures and VC

Fig. 6. RV at different temperatures and VC

2.3. Preparations of graphene nanofluids

The graphene nanofluids was prepared by dispersing graphene nanoparticles in water with Gum Arabic surfactant. The two-step method, which is the most efficient and effective technique for producing NFs, was used. The solution was stirred for 1 hour, followed by 2.5 hours of ultrasonication. No sedimentation of particles was observed for 30 days. Four VCs were prepared: 0.01%, 0.05%, 0.1% and 0.2% NFs. Fig. 7 shows that the TC of NF increases with particle concentrations and temperatures. The variations in NF viscosity as a function of nanoparticle VCs and temperature are represented in Fig.8. The viscosity of the NF decreased when the temperature was increased from 20 °C to 60 °C at the constant VC.
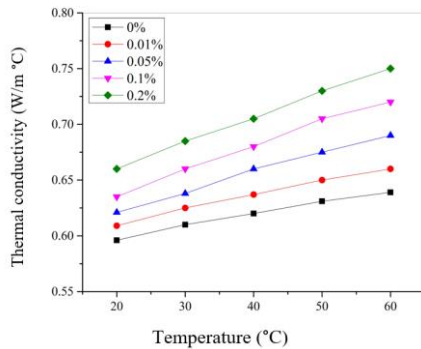

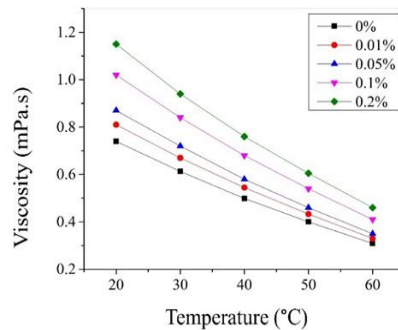Fig. 7. TCR of HNF with (a) VCs at different temperatures

Fig. 8. The viscosity at different temperatures and VCs.

Further, a new proposed correlation was obtained to measure the thermal conductivity ratio and viscosity variations at different concentrations and temperatures, we determined the TCR and RV by using Eqs. 15 and 16 at different temperatures as follows:

$$TCR = 0.9965 + 0.7082\varphi + 0.0005184T - 1.835\varphi^2 + 0.006788\varphi\ T. \quad (15)$$

$$RV = 1.059 + 3.647\ \varphi - 0.0005436\ T - 5.19\ \varphi^2 - 0.003709\ \varphi\ T. \quad (16)$$

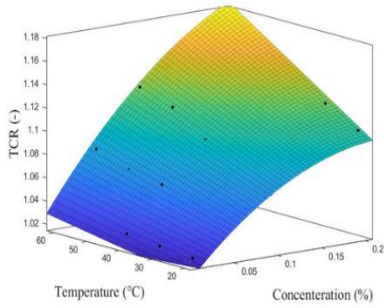Figs. 9 and 10 shows a comparison between the experimental results obtained and the proposed equation.

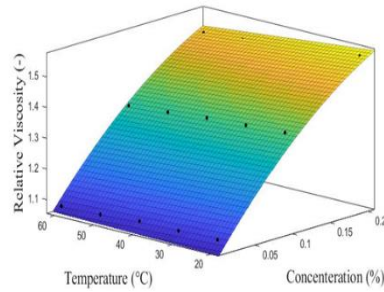Fig. 9.TCR comparisons for different temperatures and VC

Fig. 10. RV at different temperatures and VC

2.4. Preparing nanocoating

Matte acrylic coating is used in many solar applications due to its good absorbency of solar radiation and high heat resistance. Therefore, the iron oxide and graphene nanoparticles were added to the matte acrylic coating to enhance the absorption of solar radiation because of their dark black colour. Then, the coating fluid is put in a container of known volume and weight to measure the coating's density by dividing the weight by the volume. Nanoparticles of graphene- and Fe_3O_4 acrylic, which was used as the mixture's base fluid, were mixed in a 1:1 ratio to make the nanocoating. The fluid coating was put in a beaker (250 mL) and stirred for 0.5 hours. After that, it was mixed with ultrasonic waves for 0.5 hours to break up particles that were sticking together and spread them out evenly in the base fluid to make a stable nanocoating

2.5. Numerical analysis

Ansys Fluent 2020 software is used to develop and analyse the three-dimensional CFD thermal model of the single receiver tube. The heat flux

value is considered uniform on the receiver tube's surface. The following assumptions have been taken into consideration in the numerical analysis:

- In receiver tube numerical analysis with uniform heat flow, the outer surface has two parts.
- The heat transfer fluid used was water and nanofluid.
- Three-dimensional steady flow was adopted.
- Newtonian fluid.
- Incompressible fluid.
- Turbulent flow.

Several Nusselt numbers and fraction factor correlations were applied to validate the numerical model results. Heat transfer and fluid friction were validated. Water was used in all the correlations presented in Fig. 11: the Gnielinski, the Dittus–Boelter, the Pak–Cho, and the Notter–Rouse.

The friction factor of water is compared in Fig. 12 to the correlations provided by Blasius and Petukhov. The maximum deviations of the friction factor from the Gnielinski and Blasius correlations were 3.76% and 4.33%, respectively. In addition, the correlation inaccuracy in industrial applications is allowed to be 20% (Cheng et al., 2012), (Huang et al., 2017). Therefore, the results of the current study agree with the presented correlations.
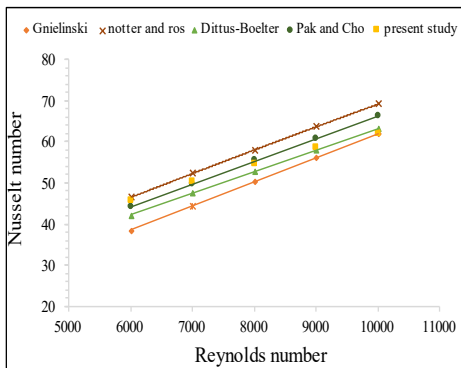

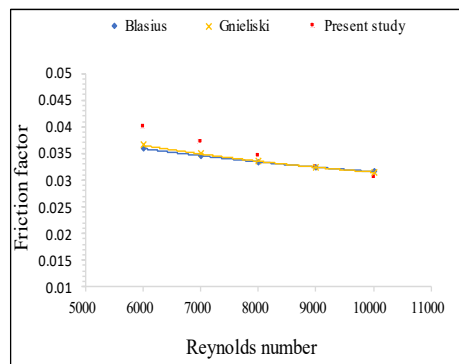Fig. 11. Nu no. validation of water using literature correlation

Fig. 12. Friction factor validation of water using literature correlation

3. RESULTS

This chapter presents the most important results obtained from the experimentation and their discussions.

3.1. Similarity tests of each collector using aluminium reflective surface and water

In the beginning, similarity tests of the two collectors were carried out using the aluminium reflective surface for each one to ensure that the two collectors worked with the same performance under the same conditions. The mass flow rate of 90 L/h was used to pass through the absorber tube. The experiments were carried out at the solar lab of the Hungarian University of Agriculture and Life Sciences from around 10:00 a.m. to 15:00 p.m. in the summer of 2022. The results showed that the average efficiencies of the upper and lower collectors were 21.382% and 21.436%, respectively. According to the test results, the average thermal efficiency (TE) between collectors did not exceed 0.3%. According to experience, the two collectors work with performances close to each other.

3.2. Effect of reflective surface on PTSC performance

This study focuses on the effect of a refractive surface on the performance and efficiency of the PTSC. Two PTSC collectors with different reflecting surfaces were created: one from silver chrome film (SCF) and the other from Aluminium sheet (AS). In addition, all collectors used water as the base fluid. To determine which is better for applications, one uses AS and the other uses SCF in the PTSC. Furthermore, the comparison is made with different mass flow rates (30 L/h, 60 L/h, 90 L/h, and 120 L/h) with an evacuated glass tube in a U shape.

The heat removal factor is represented by the ratio of the actual to the maximum heat transfer through the PTSC. The heat removal factor of water increased as the mass flow rate increased, as shown in Fig. 13. Thus, the amount of heat removal factor obtained for SCF is equal to 58.5%, 54.5%, 50.1%, and 43.1% for 120, 90, 60, and 30 L/h mass flow rates, respectively. Moreover, the amount of heat removal factor obtained for AS was 46.02%, 35.4%, 28.9, and 24.9 for 120, 90, 60, and 30 L/h mass flow rates, respectively. The collector's efficiency for each mass flow rate is presented as a function of T*. Fig. 14 compares aluminium sheets' thermal efficiencies with different flow rates. Obviously, the TE values obtained have increased as the mass flow rate increased. According to the experimental results, the maximum TE with AS was obtained at 120 L/h, 90 L/h, 60 L/h, and 30 L/h mass flow rates, reaching 27%, 22.84%, 18.9%, and 14.86%, respectively. Fig. 15

presents the thermal efficiencies obtained using SCF with different flow rates as a function of T*. The maximum TE with SCF was obtained for 120, 90, 60, and 30 L/h mass flow rates and reached 46.84%, 43.49%, 40.26%, and 33.68%, respectively. According to the results, the thermal performance of the PTSC using SCF is better than AS.
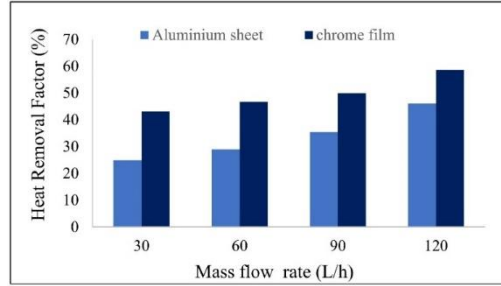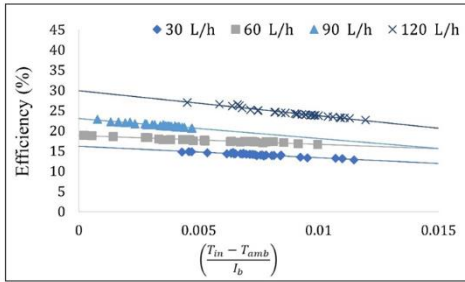

Fig. 13. Heat removal factor for SCF and AS

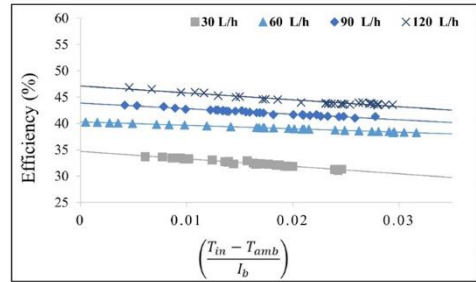Fig. 14. TE and heat loss parameter at different mass flow rates of AS

Fig. 15. TE and the heat loss parameter at different mass flow rates of SCF

3.3. Effect of receiver tube coating on PTSC performance

In typical PTSCs, the receiver is essentially one of the main and most important components of the collector. Therefore, the coating lifetime should be stable to enhance efficiency and reduce maintenance costs. Coatings are used to enhance the performance of absorbers in terms of quality, efficiency, maintenance, and cost. Different coatings are required as there are no uniformly perfect materials for various applications, working conditions, and material variations. This study focuses on the effect of a receiver tube coating on the performance and efficiency of the PTSC. Therefore, the coating method must be chosen based on the application area, availability, and cost criteria. Spray coating is a reliable method for getting good properties, highly adhesive coatings, and anticorrosive coatings over the copper tube. The sputtering coating method has a certain significance for depositing films on the substrate

and is economical and environmentally friendly method. Two PTSCs with different coatings were created: one with a nanocoating (NC) and the other with a matte coating (MC). In addition, the PTSC comparison is made with different mass flow rates (30, 60, 90, and 120 L/h). The nanocoating was prepared as described in the Materials and Methods chapter, and a single evacuated absorber tube was used in the experiment.

The heat removal factor of water increased as the mass flow rate increased, as shown in Fig. 16. Thus, the amount of heat removal factor obtained for NC is equal to 52.7%, 51.1%, 49%, and 46.2% for 120, 90, 60, and 30 L/h mass flow rates, respectively. Moreover, the amount of heat removal factor obtained for MC equals 50.3%, 49%, 48%, and 43% for 120, 90, 60, and 30 L/h mass flow rates, respectively.
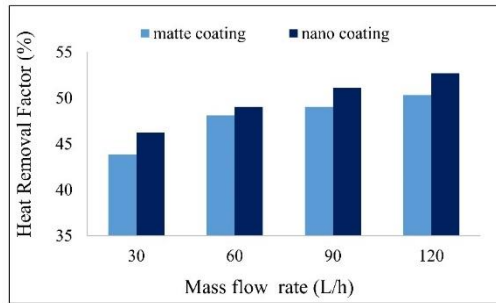

Fig. 16. Heat removal factor for NC and MC

The collector's efficiency for each mass flow rate is presented as a function of T*. Fig. 17 compares MC thermal efficiencies with different flow rates. Obviously, the TE values obtained had increased as the mass flow rate increased. According to the experiment results, the maximum TE with MC was obtained for 120, 90, 60, and 30 L/h mass flow rates and reached 40.37%, 38.39%, 37.27%, and 34.98%, respectively. Fig. 18 presents the thermal efficiencies obtained using NC with different flow rates as a function of T*. The maximum TE with NC was obtained for 120, 90, 60, and 30 L/h mass flow rates and reached 41.58%, 40.6%, 39%, and 36.88%, respectively. According to the results, the thermal performance of the PTSC using NC is better than MC. NC showed a remarkable enhancement of TE by decreasing thermal losses. Finally, the NC is more effective at improving system performance.
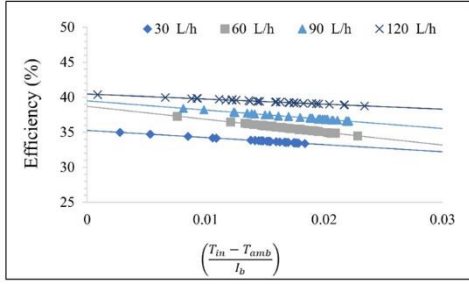
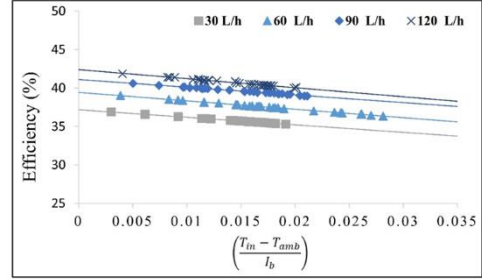Fig. 17. TE and heat loss parameter at different mass flow rates of MC

Fig. 18. TE and the heat loss parameter at different mass flow rates of NC

3.4. Test case hybrid nanofluid

This study involved manufacturing a prototype of PTSC that would be used to determine the efficiency of a working fluid made of graphene and Fe_3O_4 nanoparticles suspended in a water as a based nanofluid. The experiments were carried out with graphene–Fe_3O_4/water HNFs in different concentrations (0.01%, 0.05%, 0.1%, and 0.2%) with a mass flow rate of 120 L/h. Fig. 19 shows that the heat removal factor of HNF was higher than that of water. As observed, the heat removal factor increased as the concentration of nanoparticles increased. According to the results, the heat removal factor of the graphene-Fe_3O_4/water HNF was 57.7%, 56.3%, 53.9%, and 52.2% for 0.2%, 0.1%, 0.05%, and 0.01% VCs, respectively, while the heat removal factor with water was 51.4%.

At a 0.2% volume concentration of graphene-Fe_3O_4/water HNF, the heat removal factor reached the maximum value of 57.7%. For the base fluid (water), the heat removal factor reaches the minimum value of 51.4%. It's clear that the heat removal factors for graphene– Fe_3O_4/water HNF are higher than those for water for all examined volume concentrations. The increase in heat removal factor with increasing concentrations is due to the increased thermal conductivity resulting from the increase in nanoparticle concentration.
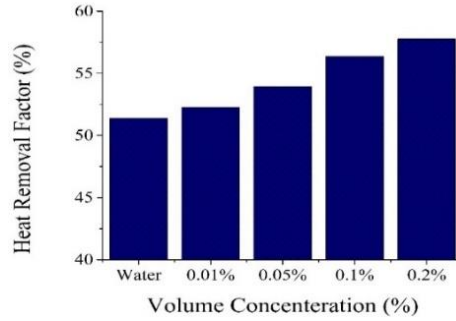
Fig. 19. Heat removal factors at different VCs and water

Fig. 20 shows the efficiency of collector changes as a function of T^* using different VCs. The collector's efficiency increased with increasing volume concentration. According to the experimental results, the maximum TE of graphene-Fe_3O_4/water HNF was obtained for 0.2%, 0.1%, 0.05% and 0.01% VCs and reached 45.46%, 44.3%, 42.04% and 41.02%, respectively, while the collector efficiency with water was 40.41%. To validate the experimental results with the simulation results, a modelling analysis and simulation using ANSYS Fleunt software was used.

According to the simulation, the maximum TE of graphene-Fe_3O_4/water HNF was obtained for 0.2%, 0.1%, 0.05% and 0.01% VCs and reached 45.44%, 44.36%, 42.32% and 42.37%, respectively, while the collector efficiency with water was 40.97%. It was observed that thermal efficiencies using nanofluids at all operating conditions was higher than base fluid. Fig. 21 shows the results of the experimental and simulation work with W and a 0.2% volume concentration of hybrid nanofluid, the efficiencies were close to each other.
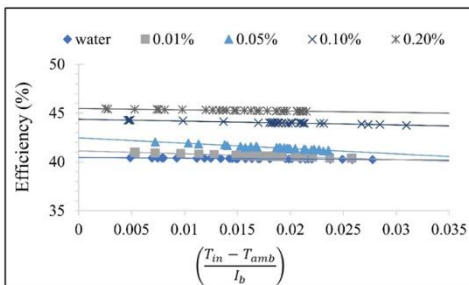

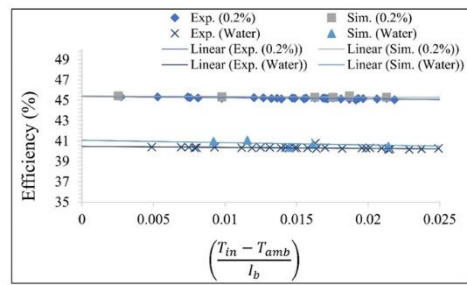Fig. 20. TE versus heat loss parameter at different VCs of G–Fe_3O_4 HNF

Fig. 21. Validation results of the numerical model with experimental data for the HNF and water

3.5. Test case graphene nanofluid

This study involved using the PTSC to determine the efficacy of a working fluid made of G nanoparticles suspended in a water based nanofluid. The

experiments were carried out with graphene/water NFs in different concentrations (0.01%, 0.05%, 0.1% and 0.2%) with a mass flow rate of 120 L/h.

Fig. 22 shows that the heat removal factor of NF was higher than the water. As observed, the heat removal factor increased as the concentration of nanoparticles increased. According to the results, the heat removal factor of the graphene–NF was 58%, 56.3%, 54% and 52.8% for 0.2%, 0.1%, 0.05% and 0.01% VCs, respectively, while the heat removal factor with W was 51.7%. At 0.2% volume concentration of graphene/water NF, the heat removal factor reached the maximum value of 58%. For base fluid (water), the heat removal factor reaches the minimum value of 51.7%. It's clear that the heat removal factors for graphene/water NF are more than water for all examined volume concentrations.
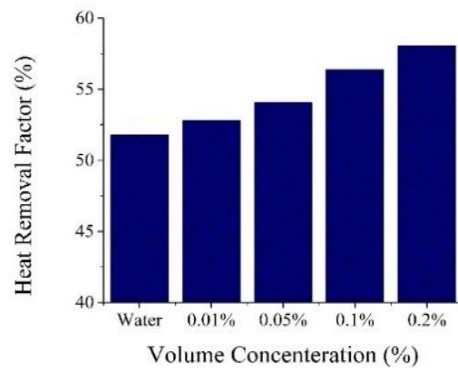

Fig. 22. Heat removal factors at different VCs and water

Fig. 23 shows the efficiency of collector changes as a function of T^* using different VCs. The collector's efficiency has increased with increasing volume concentration. According to the experiment, the maximum TE of graphene/water NF was obtained for 0.2%, 0.1%, 0.05% and 0.01% VCs and reached 44.73%, 43.97%, 42.06% and 41.23%, respectively, while the collector efficiency with water was 40.36%.

To validate the experimental results with the simulation results, a modelling analysis and simulation using ANSYS Fleunt software is used. According to the simulation, the maximum TE of graphene/water NF was obtained for 0.2%, 0.1%, 0.05% and 0.01% VCs and reached 45.75%, 44.31%, 42.26% and 42.3%, respectively, while the collector efficiency with water was 40.45%. It was observed that thermal efficiencies using nanofluids at all operating conditions was higher than base fluid. Fig. 24 shows the results of the experimental and simulation work with water and a 0.2% volume concentration of mono nanofluid, and the efficiencies were close to each other.
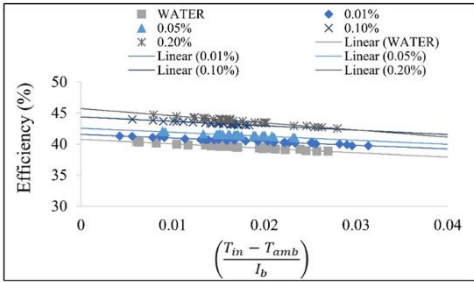
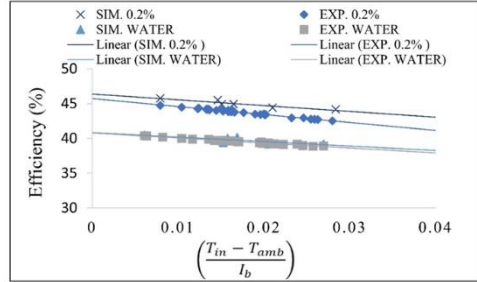Fig. 23. TE versus heat loss parameter at different VCs of graphene/water NF

Fig. 24. Validation results of the numerical model with experimental data for the graphene/water and water

3.6. The receiver geometry

The receiver geometry has influence on the optical efficiency by increasing the absorbed radiation or decreasing collector heat loss. Enhancing the thermal performance of the receiver is essential for PTSC efficiency improvement. This increases the heat transfer from the receiver's inside surface to the thermal fluid, resulting in lower heat losses and improved thermal performance. Different receivers were designed from copper material; four different cases are investigated, as they are described in Fig. 25. In addition, all cases used water as the base fluid to determine which was better for applications of PTSC. Furthermore, the comparison is made with two different mass flow rates (60 and 120 L/h).
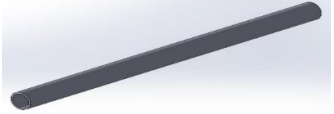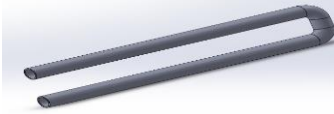
Case 1	The single evacuated absorber tube	
Case 2	Double evacuated absorber tube	
Case 3	Loop evacuated absorber tubes	
Case 4	Double evacuated absorber tube with flat plate	

Fig. 25. The four examined cases in the PTSC module

3.6.1. Performance of PTSC at (60 L/h) mass flow rate

The experiments were carried out with water in four different absorber tube designs with a mass flow rate of 60 L/h, and the required measurements were obtained and recorded. The heat removal factor of water was changed according to the absorber design, as shown in Fig. 26. Thus, the amount of heat removal factor obtained for a 60 L/h mass flow rate is equal to 65.7%, 58.1%, 50.1%, and 48.1% for cases 4, 3, 2, and 1, respectively.

Fig. 26. Heat removal factors in different cases

Fig. 27 compares thermal efficiencies in four cases at a 60 L/h mass flow rate According to the experiment results, the maximum TE for a 60 L/h mass flow rate is equal to 52.7%, 46.17%, 40.26%, and 37.27% for cases 4, 3, 2, and 1, respectively. According to the results, the thermal performance of the PTSC using a double-evacuated absorber tube with a flat plate is better than in other cases. The receiver tube showed a remarkable enhancement of TE by decreasing thermal losses.
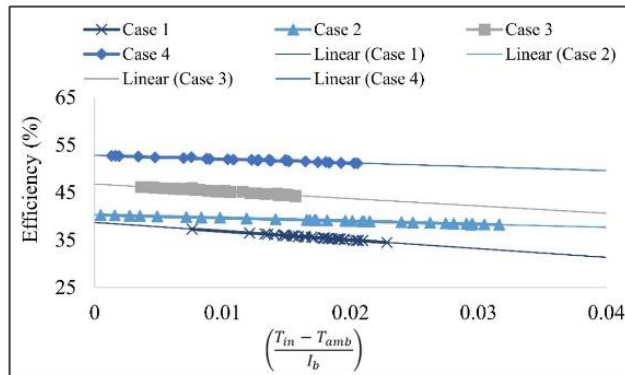
Fig. 27. TE versus heat loss parameter at different cases

3.6.1. Performance of PTSC at (120 L/h) mass flow rate

The experiments were carried out with water in four different absorber tube designs with a mass flow rate of 120 L/h. Furthermore, the TE of PTSC will be evaluated and examined in different cases. The heat removal factor of water was changed according to the absorber design, as shown in Fig. 28. Thus, the amount of heat removal factor obtained for a 120 L/h mass flow rate is equal to 73.4%, 65.8%, 58.5%, and 50.3% for cases 4, 3, 2, and 1, respectively.
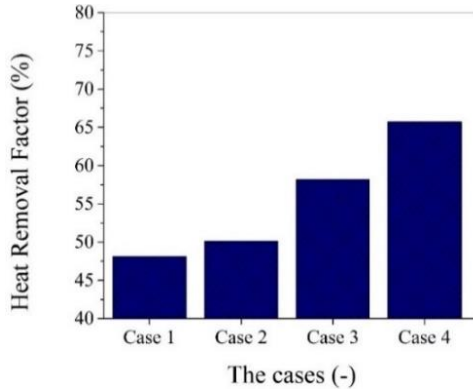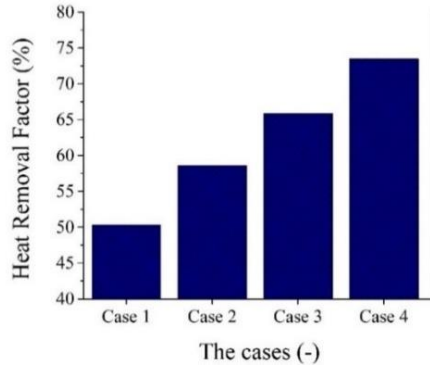

Fig. 28. Heat removal factors in different cases

Fig. 29 compares thermal efficiencies in four cases at a 120 L/h mass flow rate Obviously, the TE values obtained differ according to the design of the absorber tube. According to the experiment results, the maximum TE for a 120 L/h mass flow rate was equal to 59.05%, 52.39%, 46.84%, and 40.37% for cases 4, 3, 2, and 1, respectively. According to the results, the thermal performance of the PTSC using a double-evacuated absorber tube with a flat plate is better than in other cases. The receiver tube showed a remarkable enhancement of TE by decreasing thermal losses. Finally, the absorber tube is a more effective part for improving system performance.
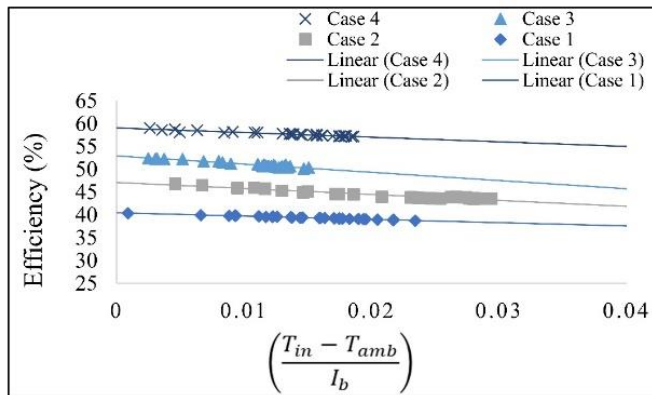
Fig. 29. TE versus heat loss parameter in different cases

19

4. NEW SCIENTIFIC RESULTS

This section presents the new scientific findings from the research as follows: work as follows:

1. *Thermal conductivity of mono and hybrid nanofluid*

Based on experimental results, I have identified a new proposed correlation for graphene/water and graphene-Fe_3O_4/water nanofluids (with GA surfactant) thermal conductivity enhancement ratios. This correlation is valid for volume concentrations ranging from 0.01% to 0.2% and temperatures ranging from 20 °C to 60 °C.

For graphene/water:

$TCR = 0.9965 + 0.7082\ \varphi + 0.000518\ T - 1.835\ \varphi^2 + 0.006788\ \varphi\ T$, R^2=0.9881.

For graphene-Fe_3O_4/water:

$TCR = 0.9994 + 0.05436\varphi + 0.00012T - 0.4568\varphi^2 + 0.01178\varphi\ T$, R^2=0.9791.

According to experimental results, the thermal conductivity of 0.2% graphene-Fe_3O_4/water was evaluated at 60 °C and observed it was 14.4% higher than the thermal conductivity of the base fluid. And graphene/water nanofluid, I have observed that the thermal conductivity of 0.2% graphene/water at 60 °C was 17% higher than the thermal conductivity of the base fluid.

2. *Viscosity of mono and hybrid nanofluid*

Based on experimental results, I have identified a new proposed correlation for measuring the relative viscosity of graphene/water and graphene-Fe_3O_4/water nanofluids with GA surfactant. This correlation is valid for volume concentrations ranging from 0.01% to 0.2% and temperatures ranging from 20 °C to 60 °C.

For graphene /water:

$$RV = 1.059 + 3.647\varphi - 0.0005436T - 5.19\varphi^2 - 0.003709\varphi\ T,$$
$$R^2\text{=0.9744.}$$

For graphene-Fe_3O_4/water:

$$RV = 1.044 + 1.889\varphi - 0.0006066T - 0.6786\varphi^2 - 0.001685\varphi\ T,$$
$$R^2\text{=0.99.}$$

3. *Effect of mono and hybrid nanofluid with surfactant on the PTSC efficiency*

I have developed and evaluated a new test rig of two identical PTSC collectors: one uses water as a working fluid, and the other uses graphene/water and graphene-Fe_3O_4/water nanofluids with Gum Arabic surfactant with different concentrations (0.01%, 0.05%, 0.1%, and 0.2%) and a mass flow rate of 120 L/h.

Based on experimental results, I identified that all cases investigated under the same conditions showed that the performance of mono- and hybrid-nanofluids is preferable to use in parabolic collector systems than the water, increasing efficiency and the output temperature of the PTSC.

Based on experimental results, the maximum thermal efficiency of PTSC for graphene-Fe_3O_4/water hybrid nanofluid was obtained for 0.2% volume concentration, reaching 45.46%, and the maximum thermal efficiency of PTSC for graphene/water nanofluid was obtained for 0.2% volume concentration, reaching 44.73%.

4. *Numerical analysis of PTSC performance*

I have developed an appropriate ANSYS Fluent Simulation Model like the experiment model in dimensions in order to investigate the convection heat transfer coefficient and hydrodynamic behaviours of mono and hybrid nanofluids by calculating the output temperature and efficiency of PTSC. The heat transfer coefficient results showed a notable increase by increasing the concentrations.

The ANSYS Fluent numerical analysis was validated using theoretical results that accounted for Nusselt and fraction factor correlations. It has been found that the results of the experimental and simulation work with water and a 0.2% volume concentration of both the graphene-Fe_3O_4/water and graphene/water nanofluids had efficiencies that were close to each other.

5. *Effect of the receiver geometry on the PTSC performance*

I have developed two novel geometry of the receiver tubes (loop evacuated absorber tube, and a double evacuated absorber tube with a flat plate) and compared them with the traditional tubes used in solar collectors. The results showed that the optical efficiency was enhanced by increasing the absorbed radiation or decreasing collector heat loss. In addition, all cases used water as the base fluid.

Based on the experimental findings, I have observed that the maximum heat removal factor obtained for 120 L/h mass flow rate was about 73.4% for the

case of a double evacuated absorber tube with a flat plate, and the maximum thermal efficiency of the PTSC with double-evacuated absorber tube with flat plate at 120 L/h was 59.05%. Conclusively, the PTSC's thermal performance using loop-evacuated and double-evacuated absorbers with flat plates was more effective than that of traditional tubes, regardless of mass flow rate.

6. *Effect of the absorber coating*

I have developed and prepared a novel nanocoating by adding iron oxide and graphene nanoparticles to the matte acrylic coating at a 0.2% volume concentration. Based on experimental results, the PTSC thermal performance using nanocoating film is preferable to use in parabolic collector systems than the matte acrylic coating, regardless of mass flow rate.

Based on experimental results, I have observed that the heat removal factor of water increased as the mass flow rate increased and the maximum heat removal factor of PTSC for nanocoating at 120 L/h was 52.7%, and the maximum thermal efficiency of PTSC for nanocoating at 120L/h was 41.58%.

7. *Effect of the reflective surface on the PTSC performance*

I have proposed a novel reflective surface for two identical PTSC collectors: one based on silver chrome film and the other on aluminium sheet. According to the experimental results, I have observed that the maximum heat removal factor and maximum thermal efficiency of PTSC for silver chrome film were, respectively, 58.5% and 46.84% at 120 L/h.

Based on experimental results, I found out that the PTSC thermal performance of silver chrome film is preferable to that of aluminium sheet in parabolic collector systems, regardless of working fluid mass flow rates.

5. CONCLUSION AND SUGGESTIONS

An experimental evaluation has been conducted to determine the performance of a novel parabolic trough solar collector using different reflecting surfaces, coating, tube designs, mono nanofluid, and hybrid nanofluid. Two identical PTSC systems were designed, manufactured, installed, and tested under the climatic conditions of at the Hungarian University of Agriculture and Life Sciences in Hungary.

In the beginning, similarity tests of the two collectors were carried out using aluminium reflective surfaces for each one with a mass flow rate of 90 L/h. It was found that the average thermal efficiency between collectors did not exceed 0.3%. During the experimental periods, the data was collected for solar radiation and temperatures (ambient, inlet, and outlet temperatures) for use them in the boundary conditions in the ANSYS software. Further, the temperature difference decreased as the flow rate through the absorber tube increased.

The reflective surface material of the PTSC greatly influenced its performance and efficiency. The silver chrome film has superior optical properties compared to regular aluminium reflective surfaces. The maximum thermal efficiency of PTSC for silver chrome film at 120 L/h was 46.84%.

Adding iron oxide and graphene nanoparticles to the matte acrylic coating has increased the amount of radiation absorption. Thus improved the optical and thermal efficiency of PTSC.

Four different receivers were designed from copper material, and four different cases were investigated. According to the results, the maximum thermal efficiency of PTSC for cases 4, 3, 2, and 1 at 120 L/h was 59.05%, 52.39%, 46.84%, and 40.37%, respectively. Furthermore, the receiver tube has increased the optical efficiency by increasing the absorbed radiation and decreasing collector heat loss.

Nanofluids significantly improved the thermophysical properties of working fluids. The NFs improved the heat transfer performance of the absorber. In addition, increasing the volume concentration of hosted nanoparticles has enhanced the collector's thermal performance and increasing the concentration and temperature of nanofluids had improved their thermal conductivity. In all cases investigated under the same conditions, the performance of nanofluids were found to be higher than that of water, increasing the efficiency and the output temperature of the PTSC.

There are numerous recommendations for future works that can be made. Studies on different shapes of absorber tubes (e.g., elliptical cross section) and their effects on thermal efficiency and distribution of heat flux are recommended. Many areas still need to be investigated using hybrid nanofluids and mono-nanofluids.

6. SUMMARY

PERFORMANCE ANALYSIS OF A PARABOLIC TROUGH SOLAR COLLECTOR

A comprehensive performance analysis of a novel parabolic trough solar collector (PTSC) for thermal applications has been conducted. Two identical PTSC systems were manufactured, installed, and tested at the Hungarian University of Agriculture and Life Sciences in Hungary. The PTSCs were tested in the local climate of Gödöllő, Hungary in summer months. The PTSC consists of a reflecting surface, an absorber tube, and the working fluid passing through the tube.

To achieve the aim of the research, the focus was on the reflecting surface, absorber tube coating, tube design, and working fluid because they are regarded as the most important factors influencing PTSC performance. Experiments were carried out at the solar lab of the Hungarian University of Agriculture and Life Sciences from around 10:00 to 15:00.

According to the findings, surface reflectance is critical to the thermal efficiency of PTSC. The maximum thermal efficiency of PTSC with AS was obtained for a 120 l/h mass flow rate, reaching 27%. The maximum thermal efficiency of PTSC with SCF was obtained at a mass flow rate of 120 L/h, which was 46.84%. The addition of graphene-Fe3O4 nanoparticles to matte acrylic coatings resulted in a significant increase in the thermal efficiency of PTSC. The maximum thermal efficiency with NC was obtained for a 120 L/h mass flow rate and reached 41.58%. According to the results, the thermal performance of the PTSC using nanocoating is better than matte acrylic coating. Moreover, the thermal modifications in the absorber tube are able to enhance efficiency and increase the useful output. The maximum thermal efficiency for a 120 L/h mass flow rate is equal to 59.05%, 52.39%, 46.84%, and 40.37%, respectively. Accordingly, the absorber tube is a more effective part for improving system performance. The addition of nanoparticles to the working fluid is an effective method to increase the thermal energy collected and the nanofluid's thermophysical properties such as viscosity, specific heat capacity, thermal conductivity, and density. HNFs bear excellent physical characteristics as compared to mono nanofluids. The maximum TE of graphene–Fe3O4 HNF was obtained for 0.2% VCs and reached 45.46%. The maximum TE of graphene–NF was obtained for 0.2% VCs and reached 44.73%, while the collector efficiency with water was 40.41%. A numerical model is presented to predict the thermal behaviour of a PTSC with water and nanofluid. ANSYS Fluent numerical analysis was validated using theoretical results that accounted for Nusselt and fraction factor correlations. Finally, the results obtained from the numerical and experimental work were in good agreement, so they could be used to validate the numerical analysis.

7. MPORTANT PUBLICATIONS RELATED TO THE THESIS

Refereed papers in foreign languages:

1. **Al-Rabeeah Asaad Yasseen,** Farkas I**.,** Seres I. (2019): Design and experimental investigation of parabolic trough solar collector, Mechanical Engineering Letters, Gödöllő, Hungary, 19, pp. 26-32., HU ISSN 2060-3789.
2. **Al-Rabeeah Asaad Yasseen,** Seres I., Farkas I. (2021): Experimental investigation and performance evaluation of parabolic trough solar collector for hot water generation, Journal of Engineering Thermophysics, 30(3), 420 432. *https://doi.org/10.1134/S1810232821030073* (IF = 2.4)
3. **Al-Rabeeah Asaad Yasseen,** Seres I., Farkas I. (2022): Recent improvements of the optical and thermal performance of the parabolic trough solar collector systems, Facta Universitatis, Series: Mechanical Engineering, 20(1), 73–94. *https://doi.org/10.22190/FUME201106030A* (Scopus: Q1, IF= 7.9)
4. **Al-Rabeeah Asaad Yasseen,** Seres I., Farkas I (2022): Selective absorber coatings and technological advancements in performance enhancement for parabolic trough solar collector, Journal of Thermal Science, 31(6), 1990–2008*. https://doi.org/10.1007/s11630-022-1634-5* (Scopus: Q2, IF = 2.5)
5. **Al-Rabeeah A. Y,** Seres I., Farkas I. (2022): Effects of concentration and temperature on the viscosity and thermal conductivity of graphene–Fe3O4/water Hybrid nanofluid and development of new correlation, Journal of Engineering Thermophysics, 31(2), 328–339. (IF = 2.4)
6. **Al-Rabeeah Asaad Yasseen**, Seres I., Farkas I. (2023): Experimental investigation of improved parabolic trough solar collector thermal efficiency using novel receiver geometry design, International Journal of Thermofluids, p. 100344. *https://doi.org/10.1016/j.ijft.2023.100344* (Scopus: D1)
7. **Al-Rabeeah Asaad Yasseen**, Seres I., Farkas I. (2023): Experimental investigation of parabolic trough solar collector thermal efficiency enhanced with different absorber coatings, International Journal of Thermofluids, p. 100386. *https://doi.org/10.1016/j.ijft.2023.100386* (Scopus: D1)
8. **Al-Rabeeah Asaad Yasseen,** Seres I., Farkas I. (2023): Experimental investigation of parabolic trough solar collector thermal efficiency enhanced by different reflective materials, Journal of Engineering Thermophysics, Vol. 32 (3), pp. xx-xx. (IF = 2.4, accepted)

International conference proceedings:
9. **Al-Rabeeah Asaad Yasseen,** Seres I., Farkas I. (2022): Thermal improvement in parabolic trough solar collector using receiver tube design and nanofluid, in Mechanisms and Machine Science. Springer, 30–40. *https://doi.org/10.1007/978-3-030-87383-7_4*
10. **Al-Rabeeah Asaad Yasseen,** Seres I., Farkas I. (2023): Performance enhancement of PTSC by using mono and hybrid nanofluids, Proceedings of the 3rd Faculty of Industrial Technology International Congress, Bandung, Indonesia, October 28-29, 2021. pp. 67-73., ISSN 2962-1798.